Available online at www.sciencedirect.com
SCIENCE DIRECT®
Biomaterials 25 (2004) 1309–1317
Biomaterials
www.elsevier.com/locate/biomaterials

Decreased functions of astrocytes on carbon nanofiber materials

Janice L. McKenzie[a], Michael C. Waid[a], Riyi Shi[b], Thomas J. Webster[a,*]

[a] Department of Biomedical Engineering, Purdue University, West Lafayette, IN 47907, USA
[b] Basic Medical Sciences, Purdue University, West Lafayette, IN 47907, USA

Received 29 January 2003; accepted 11 August 2003

Abstract

Carbon nanofibers possess excellent conductivity properties, which may be beneficial in the design of more effective neural prostheses; however, limited evidence on their cytocompatibility properties currently exists. The objective of the present in vitro study was to determine cytocompatibility properties of formulations containing carbon nanofibers pertinent to neural implant applications. Substrates were prepared from four different types of carbon fibers, two with nanoscale diameters (nanophase, or less than or equal to 100 nm) and two with conventional diameters (or greater than 100 nm). Within these two categories, both a high and a low surface energy fiber were investigated and tested. Carbon fibers were compacted in a manual hydraulic press via a uniaxial loading cycle. Astrocytes (glial scar tissue-forming cells) were seeded onto the substrates for adhesion, proliferation, and long-term function studies (such as total intracellular protein and alkaline phosphatase activity). Results provided the first evidence that astrocytes preferentially adhered and proliferated on carbon fibers that had the largest diameter and the lowest surface energy. Based on these results, composite substrates were also formed using different weight percentages (0–25 wt%) of the nanophase, high surface energy fibers in a polycarbonate urethane matrix. Results provided the first evidence of decreased adhesion of astrocytes with increasing weight percents of the high surface energy carbon nanofibers in the polymer composite; this further demonstrates that formulations containing carbon fibers in the nanometer regime may limit astrocyte functions leading to decreased glial scar tissue formation. Positive interactions with neurons, and, at the same time, limited astrocyte functions leading to decreased gliotic scar tissue formation are essential for increased neuronal implant efficacy.

Keywords: Carbon nanofibers; Neural biomaterial; Astrocytes; Nanotechnology; Nanophase

1. Introduction

Biomaterial applications for the central nervous system have been implemented in a variety of ways. Probes are used for recording and applying electrical signals to better understand neuronal signaling, or for therapeutic uses. Other sanative applications include tissue bridging and the administration of pharmaceuticals/biomolecules either directly or through application of cells genetically modified to produce neurotrophic agents [1,2]. Advances in the treatment of diseases such as Parkinson's are promising and rely on incorporation of biomaterial applications for successful therapy [3]. Since such implants require unique biocompatibility properties to successfully integrate into specific physiological tissue, new formulations of biomaterials are currently being investigated to customize materials for these neural applications.

A biomaterial that has been standardly used for implant devices in the central nervous system is silicon. Unfortunately, silicon has been shown to induce significant glial scar tissue formation [3–5]. This gliotic response is mediated largely by astrocytes and forms at implant and injury sites [6–8]. Gliotic scar tissue is a common difficulty in the field of neural prosthetics and can cause significant impairment of implant functionality, especially with chronic implant applications. Specifically, this results in increased electrode impedance around the implant, decreased local density of neurons, and reduced axonal regeneration [4,7,9–12].

Design of synthetic biomaterials that mimic the properties of natural tissues is a promising method to minimize reactions such as the foreign body response and scar tissue formation. Physiological surfaces such as extracellular matrices that cells normally interact with are composed of nanoscale proteins. It then stands to

*Corresponding author. Tel.: +1-765-494-2995; fax: +1-765-494-1193.
E-mail address: twebster@ecn.purdue.edu (T.J. Webster).

0142-9612/$ - see front matter © 2003 Elsevier Ltd. All rights reserved.
doi:10.1016/j.biomaterials.2003.08.006

reason that cells of the body are accustomed to interacting with surfaces with a large degree of nanostructured surface roughness. In vitro studies with nanophase biomaterials have indeed shown that cells respond differently to materials with nanoscale than to micron-sized roughness [13–19].

Carbon fibers have been shown to be compatible with physiological cells and tissues [14,20–22] and nano-dimensioned fibers have excellent conductivity and high strength to weight ratios [23,24]. High conductivity is a promising property as electrical stimulation has been shown to be beneficial for nerve functions and for regeneration [25,26]. The size of carbon nanofibers contributes to their strength and high conductivity, but since their size is also in the nanometer regime, they are on the same scale as physiological proteins. Additionally, it has been shown that increasing the conductivity of a material correlates directly with a decreasing foreign body response [27]. The excellent electrical and mechanical properties of carbon nanofibers lend themselves to promising potential applications as central and peripheral neural biomaterials.

Despite this promising potential, cytocompatibility properties of carbon nanofibers pertinent for neural prostheses remain largely uninvestigated to date. The objective of this present in vitro study was to explore the cytocompatibility properties of carbon nanofibers with astrocytes to facilitate neural biomaterial design.

Composite material formulations provide a vehicle for incorporating the nanofiber properties into a convenient polymer matrix as well as maximizing fine control over material properties such as surface charge, mechanical strength, and conductivity. To this end, nanofibers were also integrated into a model polycarbonate urethane polymer matrix for this study. This thermoplastic was chosen for its biocompatible and mechanical properties. Composite matrix formulations and their cytocompatibility properties were investigated to further the objectives of this study.

2. Materials and methods

2.1. Substrates

Multiwalled carbon fibers with four different diameters (from 60 to 200 nm) that had been synthesized using catalytic and chemical vapor deposition were acquired from Applied Sciences, Inc./Pyrograf Products, Inc. (Cedarville, OH) [28]. The fibers were separated into two groups, those considered to be conventional (with diameters greater than 100 nm, specifically 125 and 200 nm), and those classified as nanophase (with diameters of 100 nm or less, specifically 60 and 100 nm). In each group of fibers a high surface energy (125–140 mJ/m^2) and low surface energy (25–50 mJ/m^2) fiber was represented. The low surface energy fiber was left as grown, and the high surface energy fiber was obtained by pyrolytic stripping of the carbon fiber to remove the outer hydrocarbon layer. Each type of carbon fiber was uniaxially pressed using a steel-tool die at 4000 psi for 3 min at room temperature to obtain a disc (1.327 cm^2 surface area) for cytocompatibility studies. The discs were then exposed to ultraviolet radiation for sterilization for 15 min.

Composites were formed from the 60 nm, high surface energy fibers and polycarbonate urethane (PCU). Compositions that varied polycarbonate urethane (Thermedics Polymer Products; PC3575A) to carbon nanofiber (CN) weight percents were used (PCU:CN—100:0, 98:2, 90:10, 75:25). Polycarbonate pellets were allowed to dissolve in chloroform for 1 h, while the carbon nanofibers were sonicated in chloroform for 1 h, and then the two solutions were mixed. This mixture was then sonicated for 1 h, poured into Teflon Petri dishes, and cured in a vacuum overnight. Discs (with a surface area of 1.327 cm^2) were cut from the polymer for cell adhesion experiments. The discs were sterilized by exposure to ultraviolet radiation for 15 min.

Borosilicate glass coverslips (Fisher Scientific) were used as reference substrates. The coverslips were degreased and sonicated sequentially with acetone and ethanol and were then etched with 1 N NaOH. Autoclaving was used for sterilization.

2.2. Substrate characterization

Scanning electron micrographs were used to assess the topography of the substrates of interest to the present study. For this purpose, samples were gold–palladium sputter-coated at room temperature. All micrographs were taken using a JEOL JSM-840 scanning electron microscope at 5 kV.

The chemical composition of the substrates' surface was assessed at the University of Washington using electron spectroscopy for chemical analysis (ESCA). These analyses were performed on a Surface Science Instruments (SSI) X-Probe instrument. A take-off angle of 55° was used for acquisitions in the outer 10 nm of the surface. Surface Physics software (Bend, OR) was used to acquire and analyze surface composition data.

Resistance of the materials of interest to the study was determined using tetrapolar electrodes with a LRC Bridge 2400. The probes were used to measure the resistance through a stack of the substrate discs and with a surface area of 1.327 cm^2 and heights varying from 0.035 to 0.124 cm each. Resistivity was calculated from the resistance and disc measurements.

2.3. Cell cultures

Rat astrocytes were obtained from American Type Culture Collection (CRL-2005) and used without

further characterization. The cells were cultured in Dulbecco's Modified Eagle Medium (DMEM; Gibco), supplemented with 10% fetal bovine serum (FBS; Hyclone), and 1% penicillin/streptomycin (P/S; Hyclone) in a standard cell culture environment (37°C, humidified, 5% CO_2/95% air). Passages numbers 32–40 were used.

2.4. Cell density—adhesion

Astrocytes in DMEM (supplemented with 10% FBS and 1% P/S) were seeded at a density of 3500 cells/cm^2 onto the substrates and were cultured in DMEM (supplemented with 10% FBS and 1% P/S) under standard cell culture conditions for 1 h. Cells were then rinsed with phosphate buffered saline (PBS) to remove nonadherent cells, fixed with formaldehyde (Fisher Scientific), and stained with Hoescht 33258 dye (Sigma). The visible cell nuclei were then counted in five random fields using fluorescence microscopy (365 excitation; 400 nm emission). The average cell count was recorded per cm^2 of sample substrate area. Experiments were run in triplicate and completed at least three different times.

2.5. Cell density—proliferation

Astrocytes in DMEM (supplemented with 10% FBS and 1% P/S) were seeded at a density of 3500 cells/cm^2 onto the substrates and were cultured in DMEM (supplemented with 10% FBS and 1% P/S) under standard cell culture conditions for 1, 3, and 5 days. Old media was replaced with fresh media every other day. After the appropriate time period, cells were rinsed with PBS to remove nonadherent cells, fixed with formaldehyde, and stained with Hoescht 33258 dye. By counting the stained nuclei using fluorescence microscopy (365 excitation; 400 nm emission), and averaging the number of cells in five random fields per cm^2 of substrate, cell density was determined. Experiments were run in triplicate and completed at least three different times.

2.6. Total intracellular protein content

Astrocytes (40,000 cells/cm^2) were seeded onto the substrates and cultured in DMEM (supplemented with 10% FBS and 1% P/S) under standard cell culture conditions for 7 and 14 days. Old media was replaced with fresh media every other day. At the end of each time period, the media was replaced with distilled water and the cells were lysed during three freeze–thaw cycles. The total intracellular protein of the lysed cells was assessed spectrophotometrically using a BCA protein assay kit (Pierce Chemical Co.) and following manufacturer's instructions. Specifically, aliquots of distilled water containing the proteins from cell lysates were incubated with a solution of copper sulfate and bicinchoninic acid for 30 min at 37°C. The absorbance of the samples was then measured at a light wavelength of 562 nm on a SpectraMax 290 (Molecular Devices, Corp.) with analysis software (SoftMax Pro 3.12; Molecular Devices, Corp.). The protein concentration (expressed in mg) was then determined from a standard curve obtained by running albumin concentrations in parallel with the samples. Experiments were run in triplicate and completed at least three different times.

2.7. Alkaline phosphatase activity

The experimental substrates were seeded with astrocytes at a concentration of 40,000 cells/cm^2 and were cultured in DMEM (supplemented with 10% FBS and 1% P/S) under standard cell culture conditions for 7 and 14 days. Media was replaced every other day. Cells were lysed as described in the total intracellular protein content section, then the method of Lowry [29] was used to resolve alkaline phosphatase activity. For this purpose, aliquots of the distilled water solution containing cellular protein were incubated with a reaction solution containing 2-amino-2-methyl-l-propanol (pH = 10.3) and *p*-nitrophenylphosphate (Diagnostic Kit #104; Sigma) at 37°C for 15 min, then the reaction was terminated with 0.05 N NaOH. Light absorbance of the samples was then measured at a wavelength of 410 nm on a SpectraMax 290 (Molecular Devices, Corp.) with analysis software (SoftMax Pro 3.12; Molecular Devices, Corp.). The alkaline phosphatase activity (expressed as nano-moles of converted *p*-nitrophenol/min or as Sigma units) was then determined from a standard curve obtained by running known *p*-nitrophenol concentrations in parallel with the samples. The alkaline phosphatase activity was normalized by total intracellular protein and substrate surface area (expressed as Sigma units/mg protein/cm^2). Experiments were run in triplicate and completed at least three different times.

2.8. Statistical analysis

Data are expressed as mean values ± SEM. Statistical analysis was performed using ANOVA methods to determine the variance of the quantitative data.

3. Results

3.1. Carbon fiber disc and composite characterization

Scanning electron micrographs at high magnification provided evidence of the varying fiber diameters (Fig. 1). The surface roughness was also visually increased on the carbon fiber discs in the nanometer regime. The scanning electron micrographs for the composites of polycarbonate urethane and 60 nm carbon fibers

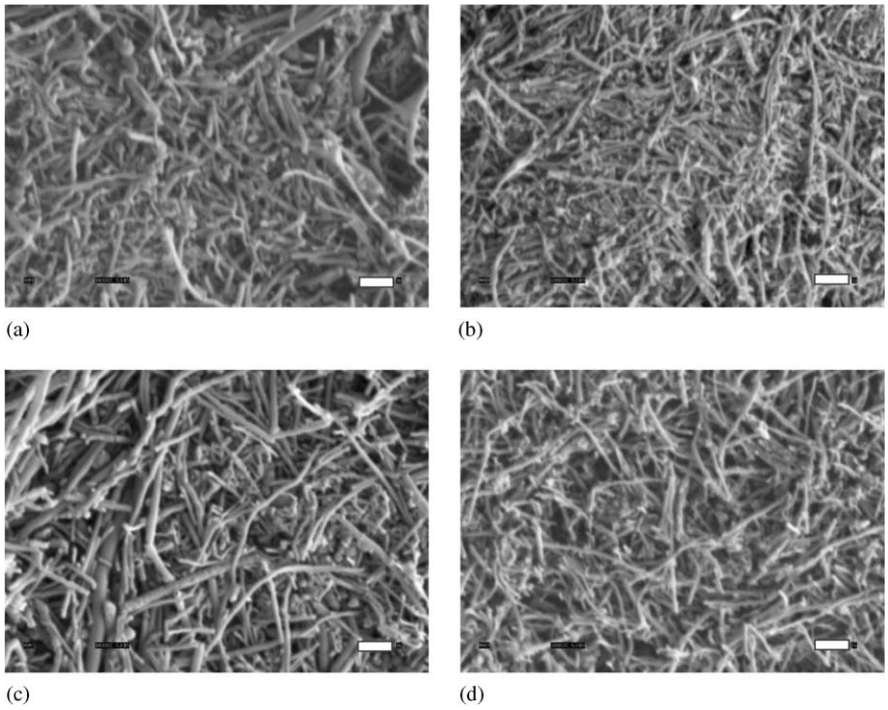

Fig. 1. High magnification scanning electron micrographs of carbon fiber discs. Representative scanning electron micrographs of the following carbon fiber discs: (a) conventional fiber with low surface energy, (b) conventional fiber with high surface energy, (c) nanophase fiber with low surface energy, and (d) nanophase fiber with high surface energy. Original magnification = 10,000 ×; 5 kV; bar = 1 μm.

revealed increasing fiber composition per increasing weight percent of carbon (Fig. 2). The fibers visibly caused an increased surface roughness in the 75:25 weight percent (PCU:CN) composite.

Electron spectroscopy for chemical analyses confirmed that the disc surfaces were composed primarily of carbon (Table 1). The results indicated the presence of small amounts of oxygen on the discs, although less was found on the high surface energy (125–140 mJ/m^2) fiber discs than on the low surface energy (25–50 mJ/m^2) discs (2.5 + 0.6–3.0 + 0.2% compared to 1.0 + 0.2–1.7 + 0.5%). The high surface energy conventional and nanophase carbon fiber discs did show a slight sulfur contamination of 0.4 + 0.1–0.5 + 0.1%, respectively.

The resistivity of the composites decreased exponentially as the weight percent of carbon nanofibers in PCU composites increased (Table 2). These values ranged from 20,500 Ω m for the 98:2 (PCU:CN wt%) composite to 0.354 Ω m for the 75:25 composite. This wide range of values indicates great flexibility in design of electrical properties for these materials by just varying the weight percentage of carbon nanofibers.

3.2. Astrocyte adhesion

After 1 h, astrocytes had preferentially adhered to the low surface energy, conventionally sized carbon fiber disc (Fig. 3). This result was significantly ($p < 0.1$) greater at 123% higher cell density than adhesion to the nanophase fiber with similar surface energy. The number of astrocytes that adhered to high surface energy fibers of both the nanophase and conventional size regimes was similar.

Adhesion to the pure polycarbonate urethane was significantly greater than to most of the composites containing the 60 nm carbon fiber (Fig. 4). In other words, substrate compositions of 90:10 and 75:25 (PCU:CN by wt%) had significantly less ($p < 0.1$) adherent cells when compared to polycarbonate urethane (100:0). The differences in adhesion between the 98:2, 90:10, 75:25, and 0:100 composites were not statistically significant.

3.3. Astrocyte proliferation

At the 1, 3, and 5 day time points, the cell density was greater on the low surface energy conventional carbon fiber disc, than on the low surface energy nanophase substrate (Fig. 5). This result was significant at each time point ($p < 0.1$ at 1 day, $p < 0.05$ at 3 days, and $p < 0.01$ at 5 days), and was up to 66% greater cell density at 5 days. Compared to the nanophase high surface energy fiber, the conventional high surface energy fiber had significantly more cells after 3 days ($p < 0.05$); more cells were on the conventional high surface energy fiber after 5 days, but this was not

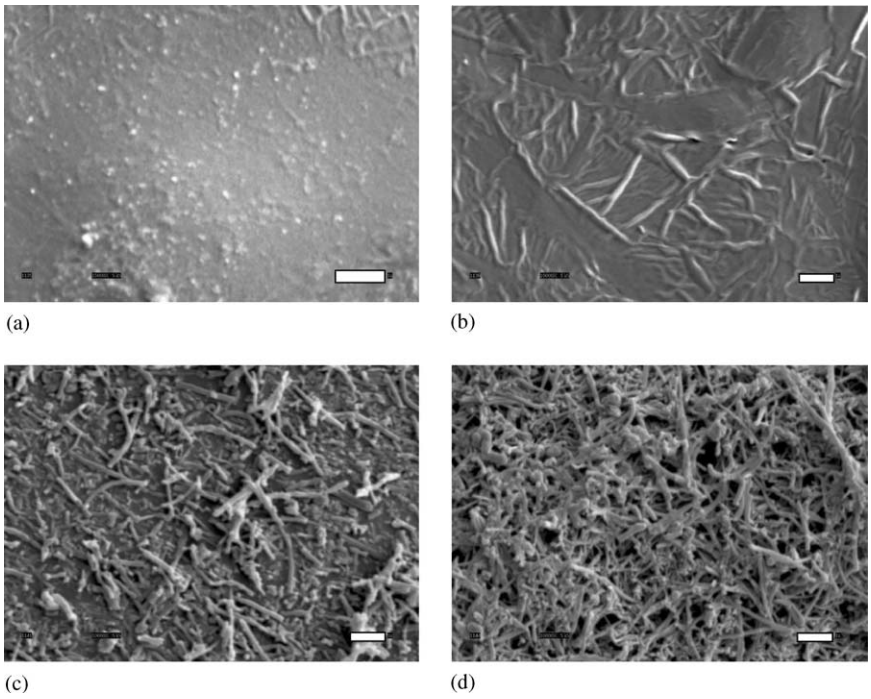

Fig. 2. High magnification scanning electron micrographs of carbon fiber composites. Representative scanning electron micrographs of varying compositions (by weight) of polycarbonate urethane (PCU) and 60 nm carbon nanophase fibers (CN) with high surface energy: (a) 100:0 (PCU:CN), (b) 98:2, (c) 90:10, and (d) 75:25. Original magnification = (a) 15,000 ×; (b)–(d) 10,000 ×; 5 kV; bar = 1 μm.

Table 1
Average composition of specific elements on carbon fibers

Type of carbon fiber	Carbon atomic percent	Oxygen atomic percent	Sulfur atomic percent
Conventional with low surface energy	97.5±0.6	2.5±0.6	nd
Conventional with high surface energy	98.6±0.1	1.0±0.2	0.4±0.1
Nanophase with low surface energy	97.0±0.2	3.0±0.2	nd
Nanophase with high surface energy	97.8±0.4	1.7±0.5	0.5±0.1

nd: Not detected.

Table 2
Resistivity of composites

Composition wt% (PCU:CN)	Resistivity (Ω m)
100:0	N/A
98:2	20,500
90:10	625
75:25	0.354
0:100	0.0598

statistically different from nanophase high surface energy fibers.

3.4. Astrocyte alkaline phosphatase activity

The alkaline phosphatase activity assay was normalized by dividing respective values of the total intracellular protein content and the substrate surface area. At 7 days, there was not a significant difference in alkaline phosphatase production between the astrocyte cells cultured on the four different carbon fibers (Fig. 6). Alkaline phosphatase production was significantly reduced at 14 days on the low surface energy, nanophase fiber when compared to the other three types of fibers ($p<0.13$ for the conventional high surface energy fiber; and $p<0.08$ for the conventional low surface energy and nanophase high surface energy fibers). Compared to all other carbon fibers, this result revealed 70–93% less of this enzyme produced on the low-surface energy carbon nanofiber.

4. Discussion

Studies have shown by staining glial scar tissue for glial fibrillary acidic protein that astrocytes often

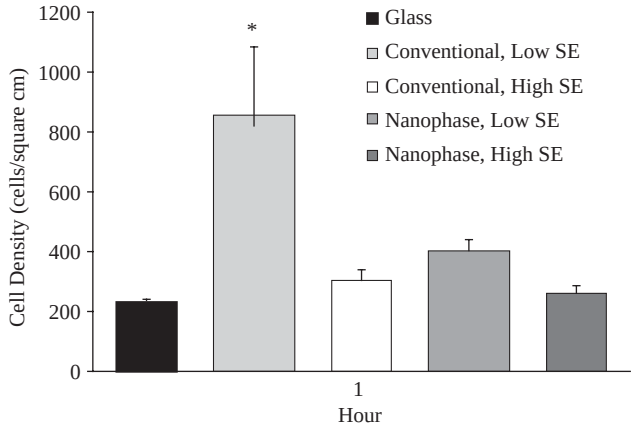

Fig, 3. Astrocyte adhesion on carbon fiber discs. Astrocytes in Dulbecco's Modified Eagle Medium (supplemented with 10% fetal bovine serum and 1% penicillin/streptomycin) were seeded (3500 cells/cm^2) and cultured on the following substrates: borosilicate glass (reference substrate), conventional fibers (200 nm) with low surface energy (SE), conventional fibers (125 nm) with high surface energy, nanophase fibers (100 nm) with low surface energy, and nanophase fibers (60 nm) with high surface energy under standard cell culture conditions for 1 h. Values are mean ± SEM; $n = 3$; $^{*}p < 0.1$ (compared to respective nanophase fiber with similar surface energy).

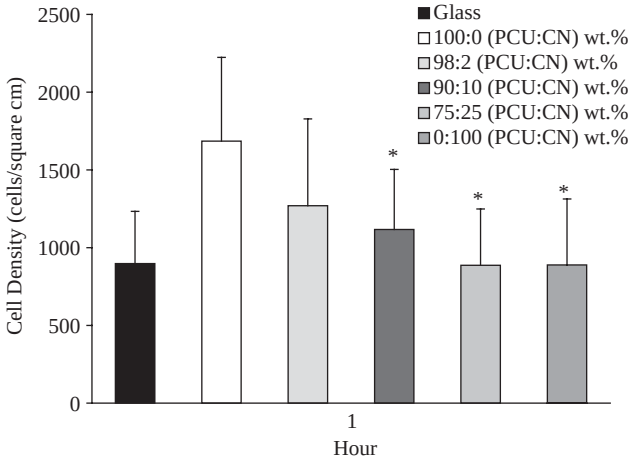

Fig. 4. Astrocyte adhesion on polycarbonate urethane and carbon fiber composites. Astrocytes in Dulbecco's Modified Eagle Medium (supplemented with 10% fetal bovine serum and 1% penicillin/streptomycin) were seeded (3500 cells/cm^2) and cultured on borosilicate glass (reference substrate) as well as on varying compositions (by weight) of polycarbonate urethane (PCU) and carbon nanophase fiber (CN; 60 nm with high surface energy) substrates: 100:0 (PCU:CN), 98:2, 90:10, 75:25, and 0:100, under standard cell culture conditions for 1 h. Values are mean ± SEM; $n = 3$; $^{*}p < 0.1$ (compared to 100:0 PCU:CN wt%).

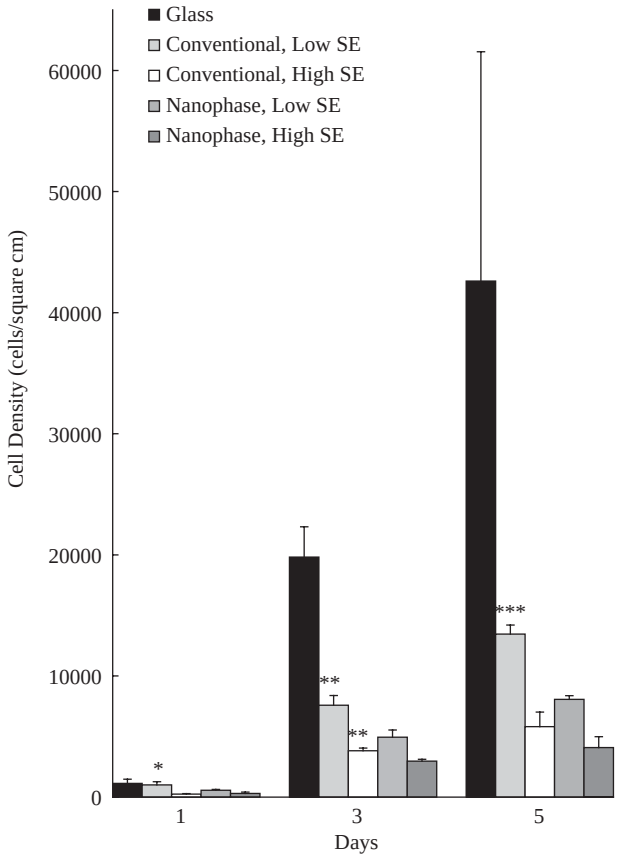

Fig. 5. Astrocyte proliferation on carbon fiber discs. Astrocytes in Dulbecco's Modified Eagle Medium (supplemented with 10% fetal bovine serum and 1% penicillin/streptomycin) were seeded (3500 cells/cm^2) on the following substrates: borosilicate glass (reference substrate), conventional fibers (200 nm) with low surface energy (SE), conventional fibers (125 nm) with high surface energy, nanophase fibers (100 nm) with low surface energy, and nanophase fibers (60 nm) with high surface energy. Astrocytes were cultured under standard cell culture conditions for 1, 3, and 5 days. Values are mean ± SEM; $n = 3$; $^{*}p < 0.1$, $^{**}p < 0.05$, $^{***}p < 0.01$ (compared to respective nanophase fiber with similar surface energy).

encapsulate traditional neural implant materials (like silicon) with non-conductive tissue [3,8]. Reducing the glial scar response, gliosis, may be possible through biomaterial design. Micropatterning is a technique that has been investigated to limit gliosis or enhance neuronal axon extension [13,30–32], but sometimes this technique includes delicate protein attachments and involves large (i.e., micronscale) surface modifications that are not able to reproduce the nanometer roughness of natural tissues. The approach of this study was to design a novel biomaterial with increased nanoscale features and without tenuous surface chemistry to decrease functions of astrocytes: carbon nanofibers. The carbon fibers designed for this study allowed for a detailed analysis of astrocyte interaction as a function of fiber dimension and surface energy. These material properties influence which specific proteins will adhere to the surface, which affects cell adhesion and interactions with the surface.

The results of this study indicated for the first time that astrocytes exhibit significantly increased cell density on low surface energy and conventionally sized (with a diameter greater than 100 nm) carbon fibers at 1 h and 1,

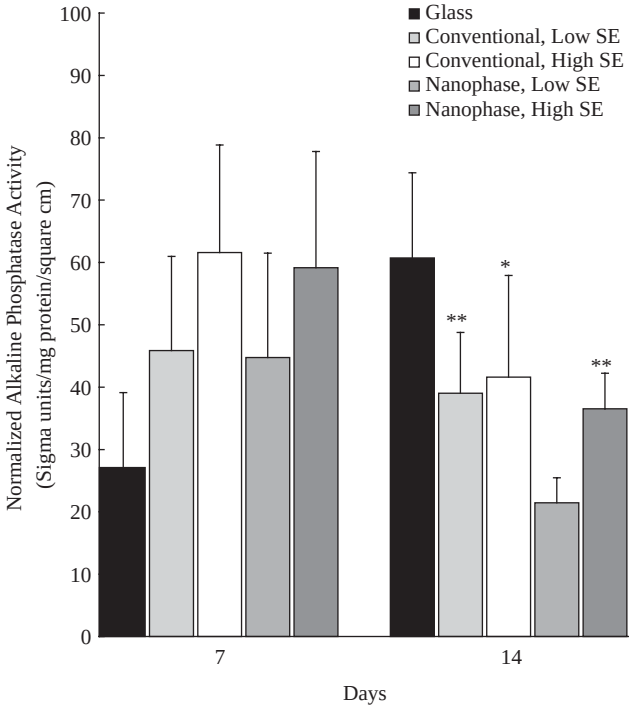

Fig. 6. Normalized astrocyte alkaline phosphatase activity on carbon fiber discs. Astrocytes in Dulbecco's Modified Eagle Medium (supplemented with 10% fetal bovine serum and 1% penicillin/streptomycin) were seeded (40,000 cells/cm^2) and cultured on the following substrates: borosilicate glass (reference substrate), conventional fibers (200 nm) with low surface energy (SE), conventional fibers (125 nm) with high surface energy, nanophase fibers (100 nm) with low-surface energy, and nanophase fibers (60 nm) with high-surface energy. Intracellular alkaline phosphatase activity (sigma units/mg protein/cm^2) was determined after 7 and 14 days. Values are mean $\pm$ SEM; $n = 3$; $^*p < 0.13$, $^{**}p < 0.08$ (compared to low surface energy nanophase fiber).

3, and 5 day time periods. Nanofibers may therefore minimize astrocyte interactions. The results of the alkaline phosphatase production study also indicated that nanophase fibers might reduce astrocytic activity even at longer time periods of 14 days.

Based on the results of the adhesion and proliferation studies for astrocytes cultured on the various carbon fibers tested, the 60 nm high surface energy carbon nanofiber was chosen for further investigation. Matrix modifications of carbon nanofibers have been shown to enhance bulk mechanical and electrical properties [23,24,33,34]. For these purposes polycarbonate urethane (PCU) was chosen as a matrix polymer. PCU has been used clinically for applications such as catheters, and has attractive mechanical properties [35–37]. The carbon nanofibers were combined with polycarbonate urethane to procure the benefits of the nanoscale carbon fibers in a more mechanically sound polymer matrix. Most of the compositions tested (90:10, 75:25; PCU:CN wt%) had significantly less adhesion of astrocytes than the pure polymer. This result confirmed the hypothesis that the nanophase carbon fiber would limit astrocyte adhesion in a polymer matrix by creating a surface with a high degree of biologically inspired nanometer roughness. Furthermore, the 75:25 composition had similar adhesion to the pure carbon nanofiber disc, and the electrical resistivity of this composite was also similar to the pure carbon nanofiber disc (0.354 compared to 0.0598 Ω m, respectively). Thus, the benefits of using PCU with carbon nanofibers can be realized with the flexibility of a range of electrical properties (such as conductivity) available for designing materials important for neural applications.

Other nanoscale materials have been fabricated in order to determine the response of neurons to the surface roughness found in native central nervous system tissues [38–41]. For example, nanostructured silicon with 10 nm pores induced positive interactions with neuronal cells in a study done by Bayliss et al. [38]. Torimitsu et al. [39] have also reported that quartz with nanoscale roughness caused greater neurite outgrowth. Similarly, polystyrene with 45 nm grooves increased neurite outgrowth [40]. More importantly for the present study, neurons have also been shown to respond positively to carbon nanotubes. Specifically, Mattson et al. [41] revealed that carbon nanofiber functionalization with 4-hydroxynonenal induced neurite outgrowth and increased neurite branching. For these reasons, the present study when considered in the context of other studies, demonstrates the strong potential nanostructured materials have to selectively increase functions of neurons; these conditions are critical to neural implant success.

5. Conclusion

In summary, this study adds to the literature by demonstrating for the first time that functions of astrocytes can be minimized on carbon nanofibers. Correlation of these results with those that have been performed using neurons with nanoscale surfaces, particularly carbon nanofibers, indicates promising interactions between neurons and nanoscale materials with potential minimization of astrocytic scar tissue formation [38–41]. As previously mentioned, nanophase carbon fibers are particularly attractive for use in neural biomaterials not only due to these special properties, but also due to their high conductivity. Further investigation of carbon nanofiber materials is necessary to verify their promise as potential neural biomaterials.

Acknowledgements

This research was funded by NSF Integrative Graduate Education and Research Training (IGERT)

Program Therapeutic and Diagnostic Devices Grant, Grant DGE-97-72770 and the NSF Research for Undergraduates (REU) Program, Grant 0097696. Special thanks to Applied Sciences, Inc./Pyrograf Products, Inc. for the carbon fibers, Dr. Stephen Golledge at the University of Washington (Department of Bioengineering, Seattle, WA) for support in surface-analysis using electron spectroscopy for chemical analysis, Ms. Beth Cardona for lab assistance, and Ms. Rachel Price for the carbon nanofiber compact scanning electron microscopy pictures (Fig. 1).

References

[1] Alexi T, Borlongan CV, Faull RLM, Williams CE, Clark RG, Gluckman PD, Hughes PE. Neuroprotective strategies for basal ganglia degeneration: Parkinson's and Huntington's diseases. Prog Neurobiol 2000;60:409–70.

[2] Park KW, Eglitis MA, Mouradian MM. Protection of nigral neurons by GDNF-engineered marrow cell transplantation. Neurosci Res 2001;40:315–23.

[3] Turner JN, Shain W, Szarowski DH, Anderson M, Martins S, Isaacson M, Craighead H. Cerebral astrocyte response to micromachined silicon implants. Exp Neurol 1999;156: 33–49.

[4] Edell DJ, Toi VV, McNeil VM, Clark LD. Factors influencing the biocompatibility of insertable silicon microshafts in cerebral cortex. IEEE Trans Biomed Eng 1992;39:635–43.

[5] Spence A, Retterer S, Isaacson M. Microfabricated model silicon probes with microfluidic channels for drug delivery. NNUN Biol Chem 2002:13.

[6] Little AR, O'Callaghan JP. Astrogliosis in the adult and developing CNS: is there a role for proinflammatory cytokines? NeuroToxicology 2001;22:607–18.

[7] Peduzzi JD, Grayson TB, Fischer FR, Geisert Jr. EE. The expression of TAPA (CD81) correlates with the reactive response of astrocytes in the developing rat CNS. Exp Neurol 1999;160: 460–8.

[8] Krum JM, Rosenstein JM. Transient coexpression of nestin, GFAP, and vascular endothelial growth factor in mature reactive astroglia following neural grafting or brain wounds. Exp Neurol 1999;160:348–60.

[9] Di Prospero NA, Zhou XR, Meiners S, McAuliffe WG, Ho SY, Geller HM. Suramin disrupts the gliotic response following a stab wound injury to the adult rat brain. J Neurocytol 1998;27: 491–506.

[10] Geisert Jr EE, Bidanset DJ, del Mar N, Robson JA. Up-regulation of a keratan sulfate proteoglycan following cortical injury in neonatal rats. Int J Dev Neurosci 1996;14:257–67.

[11] Jaworski DM. Differential regulation of tissue inhibitor of metalloproteinase mRNA expression in response to intracranial injury. Glia 2000;30:199–208.

[12] Webb K, Budko E, Neuberger TJ, Chen S, Schachner M, Tresco PA. Substrate bound human recombinant L1 selectively promotes neuronal attachment and outgrowth in the presence of astrocytes and fibroblasts. Biomaterials 2001;22:1017–28.

[13] Craighead HG, James CD, Turner AMP. Chemical and topographical patterning for directed cell attachment. Curr Opin Solid State Mater Sci 2001;5:177–84.

[14] Elias KE, Price RL, Webster TJ. Enhanced functions of osteoblasts on nanometer diameter carbon fibers. Biomaterials 2002;23:3279–87.

[15] Webster TJ, Ergun C, Doremus RH, Siegel RW, Bizios R. Enhanced functions of osteoblasts on nanophase ceramics. Biomaterials 2000;21:1803–10.

[16] Webster TJ, Ergun C, Doremus RH, Siegel RW, Bizios R. Enhanced osteoclast-like functions on nanophase ceramics. Biomaterials 2001;22:1327–33.

[17] Webster TJ, Ergun C, Doremus RH, Siegel RW, Bizios R. Specific proteins mediate enhanced osteoblast adhesion on nanophase ceramics. J Biomed Mater Res 2000;51:475–83.

[18] Webster TJ, Siegel RW, Bizios R. Design and evaluation of nanophase alumina for orthopaedic/dental applications. Nano-Struct Mater 1999;12:983–6.

[19] Webster TJ, Siegel RW, Bizios R. Osteoblast adhesion on nanophase ceramics. Biomaterials 1999;20:1221–7.

[20] Chauhan NB, Figlewicz HM, Khan T. Carbon filaments direct the growth of postlesional plastic axons after spinal cord injury. Int J Dev Neurosci 1999;17:255–64.

[21] Khan T, Dauzvardis M, Sayers S. Carbon filament implants promote axonal growth across the transected rat spinal cord. Brain Res 1991;541:139–45.

[22] Pesakova V, Klezl Z, Balik K, Adam M. Biomechanical and biological properties of the implant material carbon-carbon composite covered with pyrolytic carbon. J Mater Sci: Mater Med 2000;11:793–8.

[23] Kuriger RJ, Alam MK, Anderson DP, Jacobsen RL. Processing and characterization of aligned vapor grown carbon fiber reinforced polypropylene. Composites: A 2002;33:53–62.

[24] Lozano K. Vapor-grown carbon-fiber composites: processing and electrostatic dissipative applications. J Metals 2000;52: 34–6.

[25] Heiduschka P, Thanos S. Implantable bioelectronic interfaces for lost functions. Prog Neurobiol 1998;55:433–61.

[26] Kotwal A, Schmidt CE. Electrical stimulation alters protein adsorption and nerve cell interactions with electrically conducting biomaterials. Biomaterials 2001;22:1055–64.

[27] Seal BL, Otero TC, Panitch A. Polymeric biomaterials for tissue and organ regeneration. Mater Sci Eng R 2001;34: 147–230.

[28] www.aspci.com. Pyrograf® III. Cedarville, OH: Applied Sciences, Inc./Pyrograf Products, Inc., 2001.

[29] Lowry OH, Roberts NR, Wu ML, Hixon WS, Crawford EJ. The quantitative histochemistry of brain II. Enzyme measurements. J Bio Chem 1954;207:19–37.

[30] Ito Y. Surface micropatterning to regulate cell functions. Biomaterials 1999;20:2333–42.

[31] Kam L, Shain W, Turner JN, Bizios R. Correlation of astroglial cell function on micro-patterned surfaces. Biomaterials 1999;20:2343–50.

[32] St. John PM, Kam L, Turner SW, Craighead HG, Issacson M, Turner JN, Shain W. Preferential glial cell attachment to microcontact printed surfaces. J Neurosci Methods 1997;75: 171–7.

[33] Allaoui A, Bai S, Cheng HM, Bai JB. Mechanical and electrical properties of a MWNT/epoxy composite. Comput Sci Technol 2002;62:1993–8.

[34] Andrews R, Jacques D, Rao AM, Rantell T, Derbyshire F, Chen Y, Chen J, Haddon RC. Nanotube composite carbon fibers. Appl Phys Lett 1999;75:1329–31.

[35] www.polymertech.com/materials/bionate. Bionate polycarbonate urethane. Berkeley, CA: The Polymer Technology Group, Inc., 2002.

[36] Tanzi MC, Fare S, Petrini P. In vitro stability of polyether and polycarbonate urethanes. J Biomater Appl 2000;14: 325–48.

[37] Hergenrother RW, Wabers HD, Cooper SL. Effect of hard segment chemistry and strain on the stability of

polyurethanes: in vivo biostability. Biomaterials 1993;14: 449–58.
[38] Bayliss SC, Buckberry LD, Fletcher I, Tobin MJ. The culture of neurons on silicon. Sensors Actuators 1999;74:139–42.
[39] Torimitsu K, Furukawa Y, Tabei H. Nanostructure controlled substrates: surface modified substrates for nerve cell growth. ICCE Conference Proceedings, San Diego, CA, 2002. p. 795–6.
[40] Walsh JF, Manwaring ME, Tresco PA. Engineered adult fibroblast monolayers are capable of promoting directed outgrowth of axotomized adult neurons. Soc Biomat Conference Proceedings, Tampa, FL, 2002. p. 49.
[41] Mattson MP, Haddon RC, Rao AM. Molecular functionalization of carbon nanotubes and use as substrates for neuronal growth. J Mol Neurosci 2000;14:175–82.